ORNL/TM-2022/2494

Preliminary Thermal-Hydraulic Analysis of the UTA–2 Subcritical Linear Accelerator–Driven System

Nolan Goth
Jorge Navarro
Chris Bryan
Chad Denbrock
Robert Wahlen
Terry Grimm

June 30, 2022

OAK RIDGE National Laboratory

ORNL IS MANAGED BY UT-BATTELLE LLC FOR THE US DEPARTMENT OF ENERGY

ORNL/TM-2022/2494

Nuclear Energy and Fuel Cycle Division

PRELIMINARY THERMAL-HYDRAULIC ANALYSIS OF THE UTA–2 SUBCRITICAL LINEAR ACCELERATOR–DRIVEN SYSTEM

Nolan Goth
Jorge Navarro
Chris Bryan
Chad Denbrock
Robert Wahlen
Terry Grimm

June 30, 2022

Prepared by
OAK RIDGE NATIONAL LABORATORY
Oak Ridge, TN 37831-6283
managed by
UT-BATTELLE LLC
for the
US DEPARTMENT OF ENERGY
under contract DE-AC05-00OR22725

CONTENTS

LIST OF FIGURES

LIST OF TABLES

ACRONYMS

ADS	accelerator-driven system
CFD	computational fluid dynamics
CHT	conjugate heat transfer
DOE	U.S. Department of Energy
LEU	low-enriched uranium
ORNL	Oak Ridge National Laboratory
RANS	Reynolds-averaged Navier–Stokes

ACKNOWLEDGMENTS

The authors acknowledge Niowave Inc. for its support and collaboration during the design process.

Support for this research was provided by the US Department of Energy's (DOE's) National Nuclear Security Administration Office of Material Management and Minimization's Molybdenum-99 Program. The report was authored by UT-Battelle LLC under contract no. DE-AC05-00OR22725 with DOE.

SUMMARY

The National Nuclear Security Administration's mission includes establishing a reliable supply of ^{99}Mo without highly enriched uranium. Oak Ridge National Laboratory (ORNL) supports this objective through collaborative research and development with industrial partners. Niowave Inc., a current partner, is currently designing a subcritical linear accelerator-driven system (ADS) and preparing for the US Nuclear Regulatory Commission's licensing process. Niowave's system has the potential to efficiently supply medical radioisotopes. The technology includes a superconducting electron accelerator and a pile of both natural and low-enriched uranium (LEU) targets. The process fissions uranium and many valuable isotopes can then be extracted from the targets.

Niowave is currently iterating through conceptual and detailed design processes for several system sizes. This report discusses UTA–2, which is at the demonstration stage. UTA–2 will validate numerical modeling results with experimental measurements before progressing to the detailed design of UTA–3, the commercial-sized ADS. The thermal-hydraulic behavior of the UTA–2 core design was numerically investigated using STAR-CCM+, as described in this report. STAR-CCM+, a state-of-the-art computational fluid dynamics (CFD) software that was commercially developed by Siemens, has an extensive user base and a set of validation studies. It is also compliant with the American Society of Mechanical Engineers' Nuclear Quality Assurance 1 standard.

Three cases are investigated in this report. Case 1 quantified the temperature field within the UTA–2 assembly and water tank using only conduction as the method of thermal energy transport. This simplified approach was overly conservative and yielded wetted cladding temperatures above the coolant saturation temperature. In this case, the maximum temperature of the wetted cladding surface of the highest power rod exceeded the saturation temperature of water by 63.8°C.

Because of the overly conservative approach taken in Case 1 and its negative subcooled margin, buoyancy-driven natural circulation flow physics were implemented in Case 2. Adding coolant motion significantly distributed the thermal energy of the system through convective heat transfer. This relatively small amount of convective heat transfer significantly reduced system temperatures and increased the subcooled margin from –63.8 to 61.3°C. This margin confirmed that no boiling was expected during normal operation of UTA–2 at 230 W.

Case 3 had no additional physics models but considered an overpower event during which the power of each LEU and natural uranium rod was at its respective peak values. This resulted in a study with the total assembly power equal to 176% of the nominal power of 230 W considered in Cases 1 and 2. The resulting natural circulation flows were slightly enhanced. The subcooled margin decreased slightly to 46.3°C, which is still a significant margin to local boiling of the water within the tank. This margin confirmed that no boiling was expected during an abnormal operation of UTA–2 at 406 W.

1. INTRODUCTION

The National Nuclear Security Administration's mission includes establishing a reliable supply of ^{99}Mo without highly enriched uranium. Oak Ridge National Laboratory (ORNL) supports this objective through collaborative research and development with industrial partners. Niowave Inc., a current partner, is currently designing a subcritical linear accelerator-driven system (ADS) and preparing for the US Nuclear Regulatory Commission's licensing process. Niowave's system has the potential to efficiently supply medical radioisotopes. The technology includes a superconducting electron accelerator and a pile of both natural and low-enriched uranium (LEU) targets. The process fissions uranium and many valuable isotopes can then be extracted from the targets.

Niowave is currently iterating through conceptual and detailed design processes for several system sizes. This report discusses UTA–2, which is at the demonstration stage. UTA–2 will validate numerical modeling results with experimental measurements before progressing to the detailed design of UTA–3, the commercial-sized ADS. The thermal-hydraulic behavior of the UTA–2 core design was numerically investigated using STAR-CCM+, as described in this report. STAR-CCM+, a state-of-the-art computational fluid dynamics (CFD) software that was commercially developed by Siemens, has an extensive user base and a set of validation studies. It is also compliant with the American Society of Mechanical Engineers' Nuclear Quality Assurance 1 standard.

Three cases are investigated in this report. Table 3 summarizes the numerical results of each case. Case 1 quantified the temperature field within the UTA–2 assembly and water tank using only conduction as the method of thermal energy transport. This simplified approach was overly conservative and yielded wetted cladding temperatures above the coolant saturation temperature. In this case, the maximum temperature of the wetted cladding surface of the highest power rod exceeded the saturation temperature of water by 63.8°C.

Because of the overly conservative approach taken in Case 1 and its negative subcooled margin, buoyancy-driven natural circulation flow physics were implemented in Case 2. Adding coolant motion significantly distributed the thermal energy of the system through convective heat transfer. This relatively small amount of convective heat transfer significantly reduced system temperatures and increased the subcooled margin from –63.8 to 61.3°C. This margin confirmed that no boiling was expected during normal operation of UTA–2 at 230 W.

Case 3 had no additional physics models but considered an overpower event during which the power of each LEU and natural uranium rod was at its respective peak values. This resulted in a study with the total assembly power equal to 176% of the nominal power of 230 W considered in Cases 1 and 2. The resulting natural circulation flows were slightly enhanced. The subcooled margin decreased slightly to 46.3°C, which is still a significant margin to local boiling of the water within the tank. This margin confirmed that no boiling was expected during an abnormal operation of UTA–2 at 406 W.

2. THERMAL-HYDRAULIC ANALYSIS

This section presents the results from three cases.

1. **Case 1:** Normal operation at 100% power of 230 W and a heat removal pathway of only conduction through the system.

2. **Case 2:** Normal operation at 100% power of 230 W and a heat removal pathway of both conduction and convection through the system.

3. **Case 3:** Abnormal operation at 176% power of 406 W and a heat removal pathway of both conduction and convection through the system.

2.1 MOTIVATION

To predict the thermal margins associated with coolant boiling or damaging of the targets, an effort was needed to quantify the temperature field within the system for normal and abnormal operation.

2.2 NUMERICAL METHOD

The numerical effort consisted of performing high spatial resolution Reynolds-Averaged Navier–Stokes (RANS)–based CFD simulations. The computational tool used in this effort was STAR-CCM+ 2020.1.1, a commercial finite-volume CFD software package developed by Siemens. This finite volume approach to conjugate heat transfer uses state-of-the-art numerical methods to quantify thermal-hydraulic behavior. A RANS-based approach to turbulence modeling was chosen for this effort given the size of the domain of interest and the available computational resources. This approach was chosen to maximize the accuracy of the numerical solution for conjugate heat transfer while balancing the relative computational cost to porous media, large-eddy simulation, and direct numerical simulation methods.

2.2.1 Computational Domain

The UTA–2 core was explicitly represented with a square lattice of LEU central rods and natural uranium peripheral rods. The core was positioned within a cylindrical aluminum tank with an internal radius of 0.5 m and height of 0.83 m. A water level of 80% was established within the tank. The remaining internal volume of the tank was filled with air. Side and top views of the tank and assembly are presented in Figure 1.

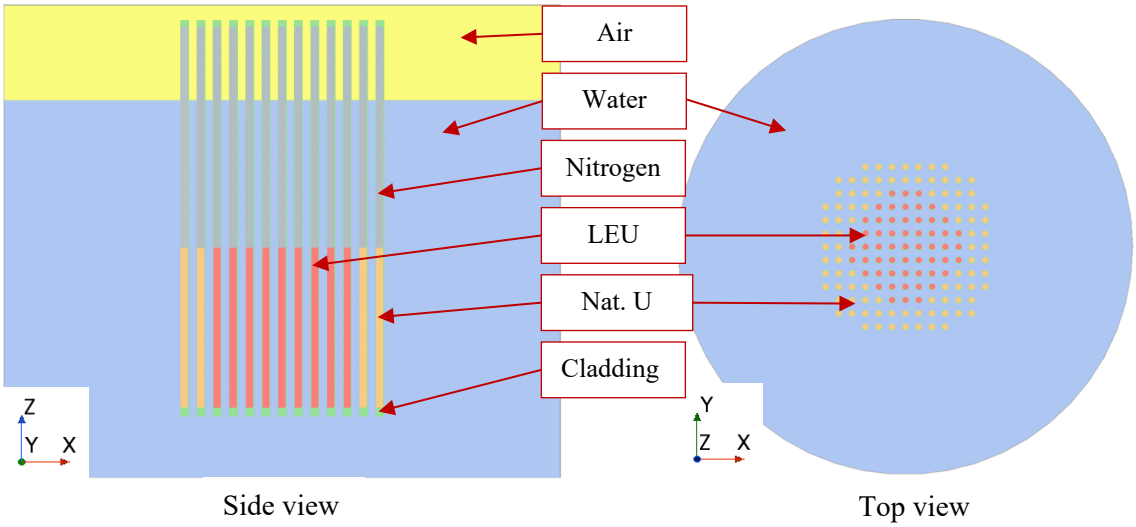

Figure 1. Side (left) and top (right) views of the UTA–2 subcritical assembly with cladding (green), LEU rods (red), natural uranium rods (orange), and water (blue). A thin grey shell enveloped the water to form the tank and perimeter of the computational domain.

The LEU and natural uranium rod are presented in Figure 2. Each rod was modeled as a lower cylinder of either LEU and natural uranium fuel and an upper cylinder of nitrogen fill gas encompassed by a cladding tube with end caps. To simplify the model and reduce the computational expense, the typical gas gap between the fuel and cladding was not included. In this effort, the conductive energy pathway was directly from the fuel to the cladding with no contact resistance. Future work will include a gap conductivity model once fabrication tolerances are defined. Contact resistance between all solid internal interfaces was neglected at this time.

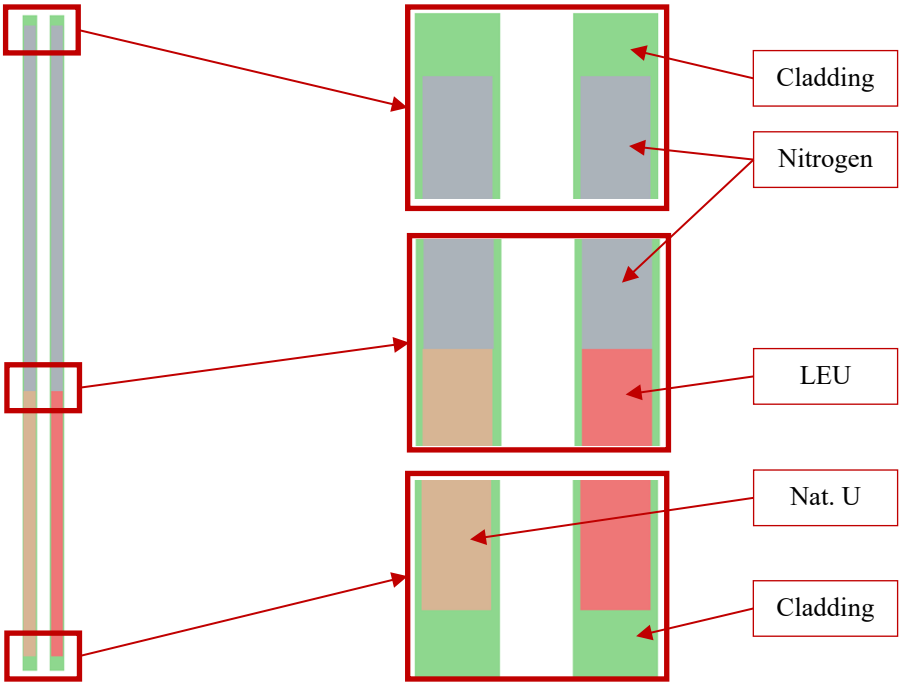

Figure 2. Cross-sectional view of natural uranium (left) and LEU (right) rods including the rod cladding (green), LEU (red), natural uranium (orange), and nitrogen fill gas (grey).

Transparent and cross-sectional views from an isometric orientation are presented in Figure 3. Because the perimeter of the computational domain was the tank exterior, thermal boundary conditions were specified on these surfaces. The vertical wall of the tank was specified as the only surface for heat removal from the tank. This is a conservative approach because the total surface area for cooling will be greater during operation and thus further reduce temperatures. A convective heat transfer boundary condition was applied to the vertical wall. The thermal specification included a bulk fluid temperature of room temperature air at 22°C surrounding the UTA–2 assembly and a convective heat transfer coefficient of 5 W/m^2-K. The technical basis for this value was established in prior experimental and computational efforts of natural circulation cooling of air flow for vertical surfaces heated 20–30°C above room temperature [1], [2]. The bottom and top lid of the tank were specified as adiabatic. The rod loading alignment guides, support plates, support stand, and beam port were neglected in this effort.

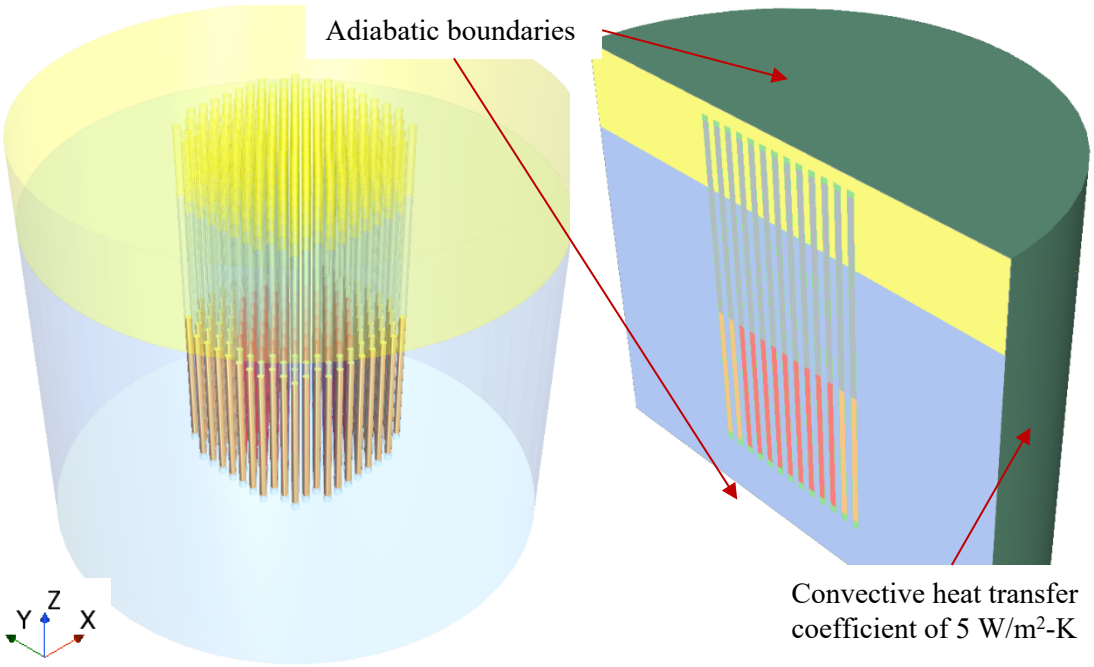

Figure 3. Transparent (left) and cross-sectional (right) isometric views of the UTA–2 subcritical assembly with cladding (green), LEU rods (red), natural uranium rods (orange), water (blue), and a tank (grey). The vertical wall of the tank was the only heat sink surface.

2.2.2 Energy Source Mapping

The energy source for each rod was defined according to the UTA–2 fission distribution provided in Figure 4 with 83.06% of the power derived from LEU rods and the remaining 16.94% derived from natural uranium rods. The total core power was 230 W for Cases 1 and 2 and 406 W for Case 3. For the preliminary design in this effort, the fueled region of each target was assigned with a spatially constant energy source. The final design will incorporate a discretized energy source to include radial, axial, and azimuthal power production distributions within each fueled region. These will be determined using a Monte Carlo N-Particle model and appropriate tally volumes.

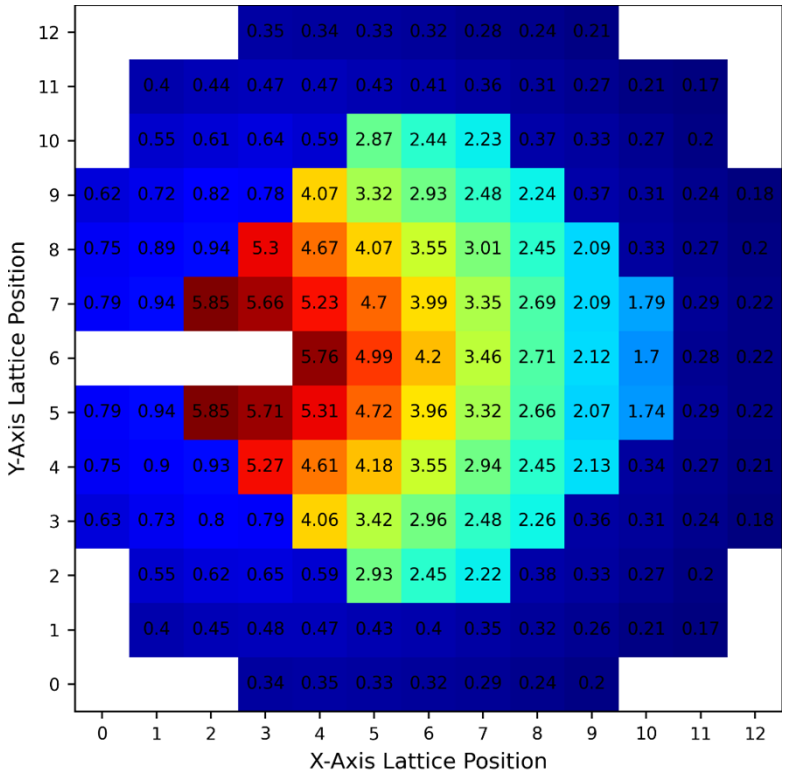

Figure 4. UTA–2 core fission power distribution during normal operation at 230 W.

2.2.3 Material Properties

Because of the anticipatedly small temperature rise above 22°C throughout the domain, constant thermophysical properties within the solid regions were considered acceptable. For the LEU and natural uranium regions, thermophysical properties of U_3O_8 were specified at 22°C [3], [4]. For the cladding and tank, values for 6061-T6 aluminum alloy at 22°C were specified [5]. For target rod fill gas, nitrogen was specified [6]. For the tank gas plena above the coolant/moderator, air was specified [7]. Table 1 presents these temperature-independent values. For the coolant/moderator, the IAPWS-IF97 database provided a temperature-dependent set of properties for water [8].

Table 1. Thermophysical properties used in the fuel, cladding, and tank regions of the domain.

Region	Material	Density (kg/m^3)	Specific heat (J/kg-K)	Thermal conductivity (W/m-K)	Dynamic viscosity (Pa s)	Molecular weight (kg/kmol)
LEU	U_3O_8	8,390	275	2.1	N/A	N/A
Natural U	U_3O_8	8,390	275	2.1	N/A	N/A
Clad	6061-T6	2,702	903	237.0	N/A	N/A
Fill gas	N_2	1.145	1,041	0.0256	N/A	N/A
Plena	Air	Ideal gas	1,004	0.0260	1.855×10^{-5}	28.966
Tank	6061-T6	2702	903	237.0	N/A	N/A

2.2.4 Numerical Solvers

For the fluid regions, 3D gradients, a steady time scheme, laminar flow, segregated flow, and segregated fluid temperature models were specified. For the solid regions, 3D gradients, a steady time scheme, and segregated solid energy models were specified.

2.2.4.1 Domain discretization

Three meshes—coarse, medium, and fine—were investigated. All meshes were fully conformal and of the polyhedral element type. The coarse, medium, and fine meshes comprised 11, 25, and 56 million volumetric elements, respectively. Cell counts within each region are specified in Table 2. Figure 5 illustrates the domain discretization within the assembly and associated water tank for the fine mesh. Conformality between solid and fluid regions is desirable as part of any conjugate heat transfer meshing strategy because this condition achieves a 1:1 face match along the interfacial surface. The conformal match ensures that the energy solvers for the solid and fluid regions communicate across all faces along the interface with no interpolate error induced.

Table 2. Number of volumetric elements in each region for the fine mesh.

Region	Volumetric elements
LEU	1.9×10^6
Natural U	3.1×10^6
Clad	10.3×10^6
Tank	1.5×10^6
Nitrogen	6.9×10^6
Water	25.9×10^6
Air	7.3×10^6
Total	56.9×10^6

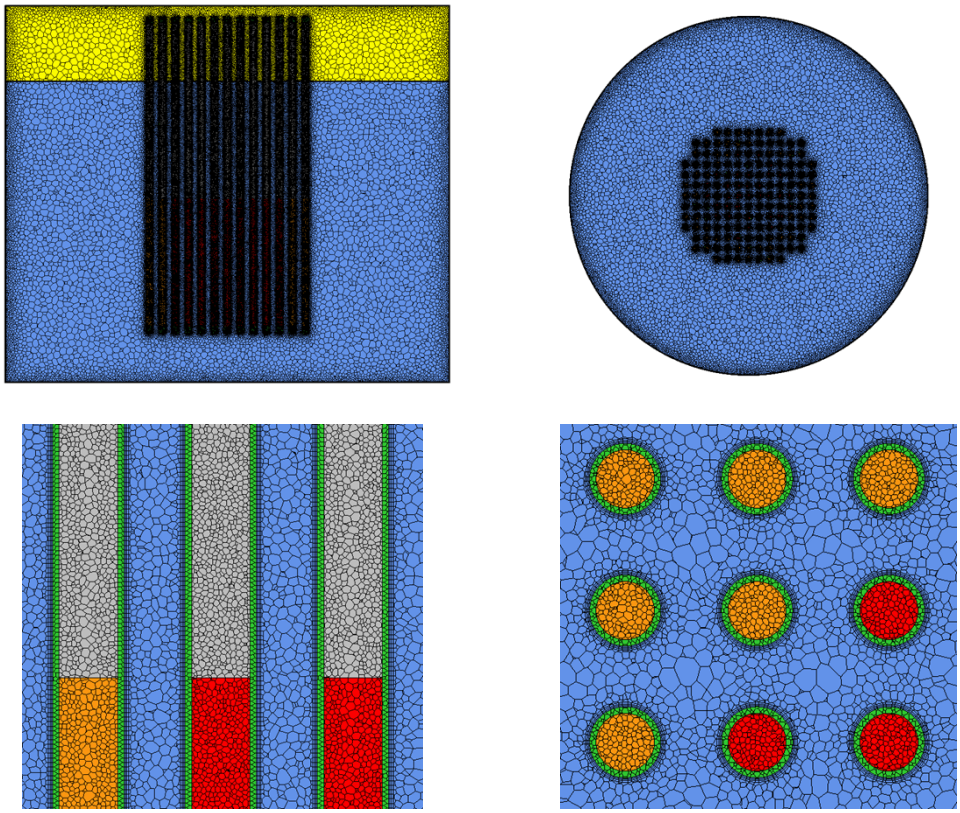

Figure 5. Domain discretization using 56 million volumetric elements and a fully conformal polyhedral mesh.

To estimate the rate of grid convergence, quantify the numerical discretization error, and determine an acceptable mesh density for Case 2 with buoyancy-induced flow, the Richardson extrapolation technique [9], [10] was applied to this effort. The method quantifies a mesh density that generates a solution independent from the number of volumetric elements used to represent the computational model.

The quantities of interest selected for this study were the maximum fuel temperature, $T_{max,fuel}$; the maximum clad temperature, $T_{max,clad}$; the maximum coolant temperature, $T_{max,coolant}$; the average fuel temperature, $T_{avg,fuel}$; the average clad temperature, $T_{avg,clad}$; the average coolant temperature, $T_{avg,coolant}$; and the surface-averaged temperature at the interface between the clad and coolant, $T_{avg,clad/coolant}$. Global trends were determined from this convergence study. The important conclusions were that all quantities except for $T_{max,clad}$ resulted in a fine-grid numerical discretization error of less than 1.5% relative to the extrapolated solution. For $T_{max,clad}$, the fine grid error was approximately 3%.

2.3 NUMERICAL RESULTS

The numerical results discussed in this section were generated using the fine mesh from above. Table 3 summarizes the primary volume-averaged and maximum temperatures for various regions of the domain. The Case 1 solution, which used only conduction as the method of thermal energy transport, had significantly higher temperatures and a negative subcooled margin. Volume-averaged LEU and natural uranium fuel temperatures were 142.7 and 112.8°C, respectively. Case 2 included the addition of fluid motion, which further distributed the thermal energy of the system through convective heat transfer. The volume-averaged LEU and natural uranium fuel temperatures decreased to 40.7 and 40.0°C, respectively. Also, a subcooled margin of 61.3°C was available, providing a substantial margin to two-phase conditions

within the tank. Case 3 considered an overpower event during which each LEU and natural uranium rods were set to the maximum rod values of 5.85 and 0.94 W, respectively. This resulted in a power output equal to 406.35 W, or 176% of the 230 W nominal value. The subcooled margin was still 46.3°C during the overpower event.

Table 3. Temperatures of primary quantities of interest for each case.

Case	LEU T_{avg} (°C)	LEU T_{max} (°C)	Nat. U T_{avg} (°C)	Nat. U T_{max} (°C)	Clad Wet T_{max} (°C)	Coolant T_{avg} (°C)	Tank Exterior T_{avg} (°C)	Subcooled margin (°C)
1	142.7	164.4	112.8	135.1	163.8	67.8	41.9	-63.8
2	40.7	41.9	40.0	40.2	41.1	39.9	38.7	61.3
3	55.1	55.8	53.9	54.2	55.0	53.7	51.8	46.3

2.3.1 Case 1: 100% Power with Conductive-Only Heat Removal Pathway

Case 1 included conduction as the only method of thermal energy transport. The coolant motion within the tank was specified and maintained at zero velocity throughout the simulation. This conservative approach yielded higher temperatures than those expected in reality and those produced in Case 2, which considered fluid motion via natural circulation. The spatial power profile and 230 W magnitude presented in Figure 4 was set for the LEU and natural uranium power producing regions. The vertical side wall was the only heat sink boundary and was specified with a convective heat transfer coefficient of 5 W/m^2-K. The steady-state solution was considered converged when an energy balance of 9.8×10^{-4} W was achieved between the energy source and sink surfaces.

Scalar fields of temperature for Case 1 are presented in Figure 6 and Figure 7. The hottest region of the domain was within the LEU rod with largest energy source and at the midplane of the active fuel length. The surface-averaged tank exterior temperature was 41.9°C. The maximum LEU and natural uranium temperatures were 142.7 and 112.8°C, respectively. These were well below the 2,500°C melting temperature of U_3O_8 [3]. However, the maximum wetted surface temperatures of several claddings were above the coolant saturation temperature. The subcooled margin on the wetted surface of the hottest rod was –63.8°C, which indicated that the local temperature was above the coolant saturation temperature. This negative subcooled margin would result in vapor generation. This conduction-only mode of thermal energy transport was extremely conservative because the purpose of Case 1 was to start with a minimal set of conservative physics and determine whether simulating more complex flow phenomena, such as buoyancy-driven natural circulation flow, would be necessary. In conclusion, it was necessary to incorporate buoyancy.

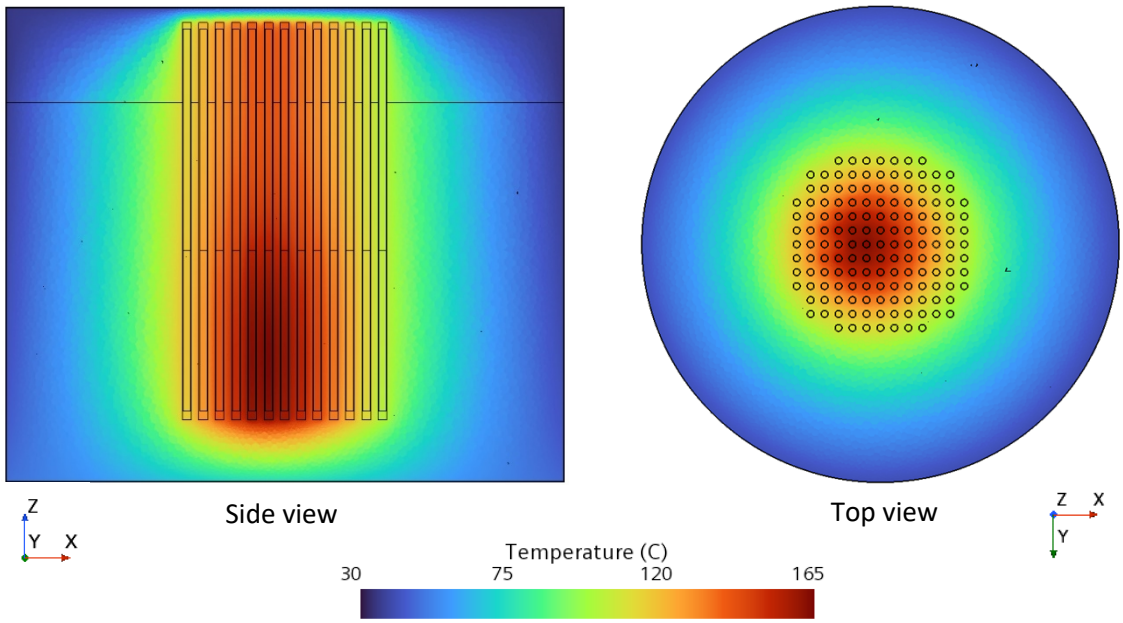

Figure 6. Side and top views of the UTA–2 subcritical assembly temperature field for Case 1 in which conduction was the only method of thermal energy transport.

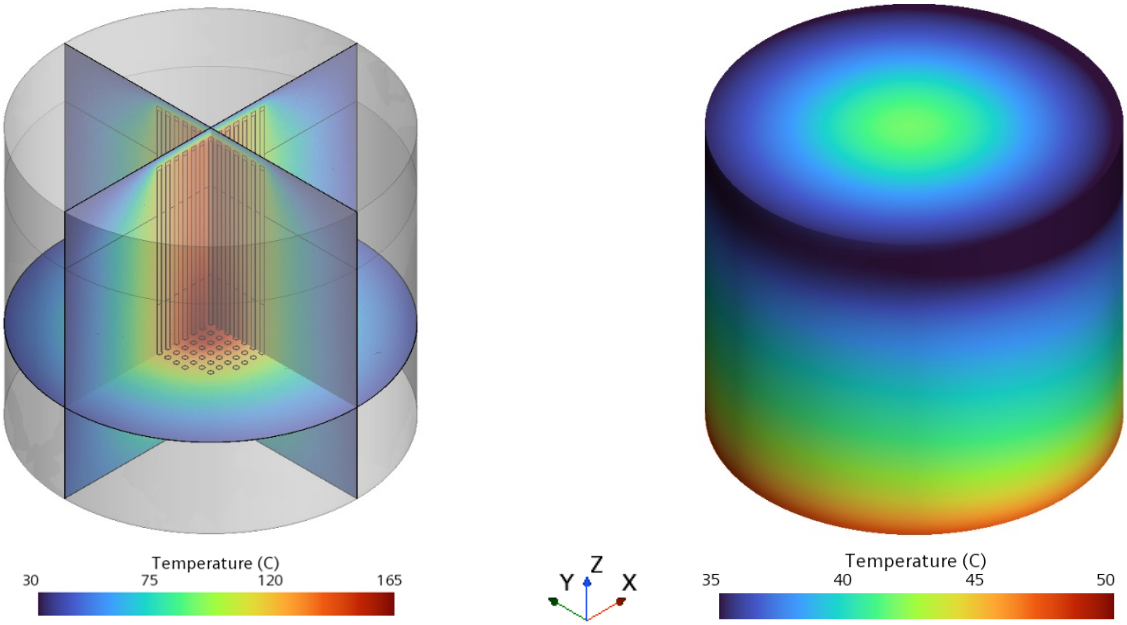

Figure 7. Isometric views of the UTA–2 subcritical assembly temperature field for Case 1 in which conduction was the only method of thermal energy transport.

2.3.2 Case 2: 100% Power with Conductive and Convective Heat Removal Pathways

Because of the negative subcooled margin of Case 1, buoyancy-driven natural circulation for the water and air regions was implemented into Case 2. Adding fluid motion distributed the thermal energy of the system via convective heat transfer. The subcooled margin was increased by 125.1°C, and the hottest clad surface was reduced from 163.8 to 41.1°C. The maximum LEU and natural uranium temperatures were 41.9 and 40.2°C, respectively. The temperature fields are presented in Figure 8 and Figure 9**.**

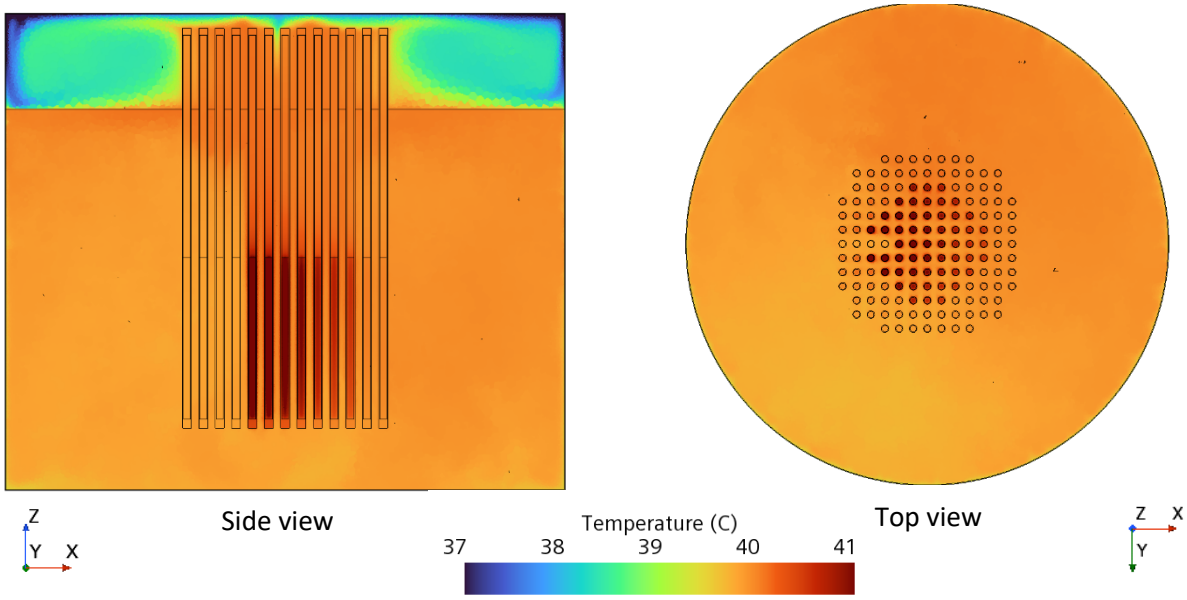

Figure 8. Side and top views of the UTA–2 subcritical assembly temperature field for Case 2 in which conduction and buoyancy-driven natural circulation were used for the normal operating condition of 230 W.

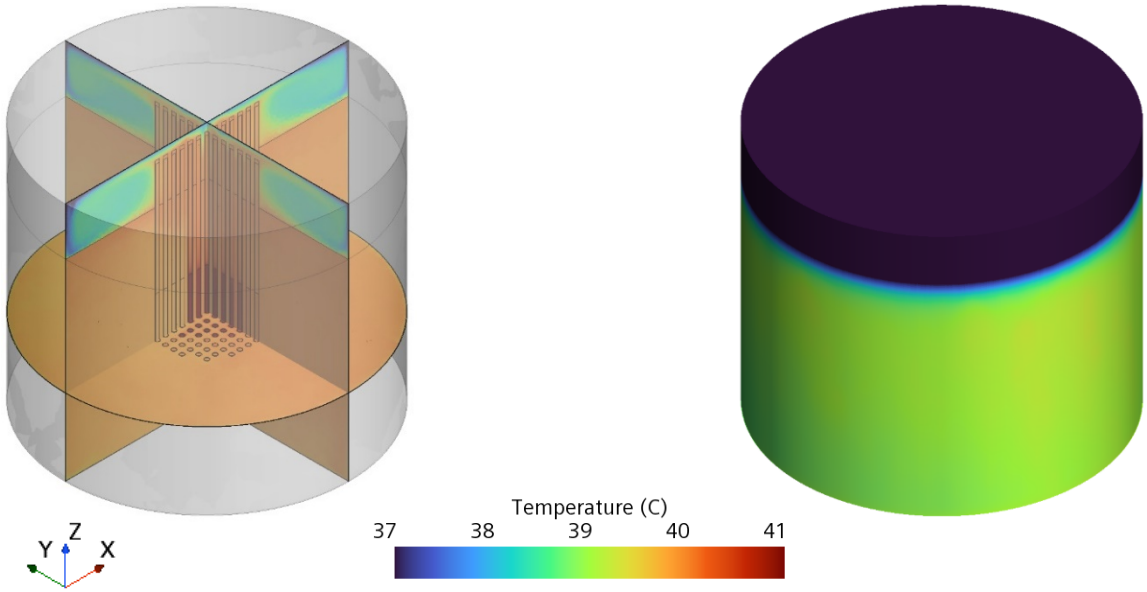

Figure 9. Isometric views of the UTA–2 subcritical assembly temperature field for Case 2 in which conduction and buoyancy-driven natural circulation were used for the normal operating condition of 230 W.

2.3.3 Case 3: 176% Power with Conductive and Convective Heat Removal Pathways

An overpower case was considered to better understand the thermal-hydraulic margin of the system. The power of each LEU rod was set to the peak LEU power-producing rod of 5.85 W located at (–2,0). The power of each natural uranium rod was set to the peak natural uranium power-producing rod of 0.94 W located at (–5,–1) and (–5,1). The total power of the assembly for this peak power case was 406 W, as shown in Figure 10.

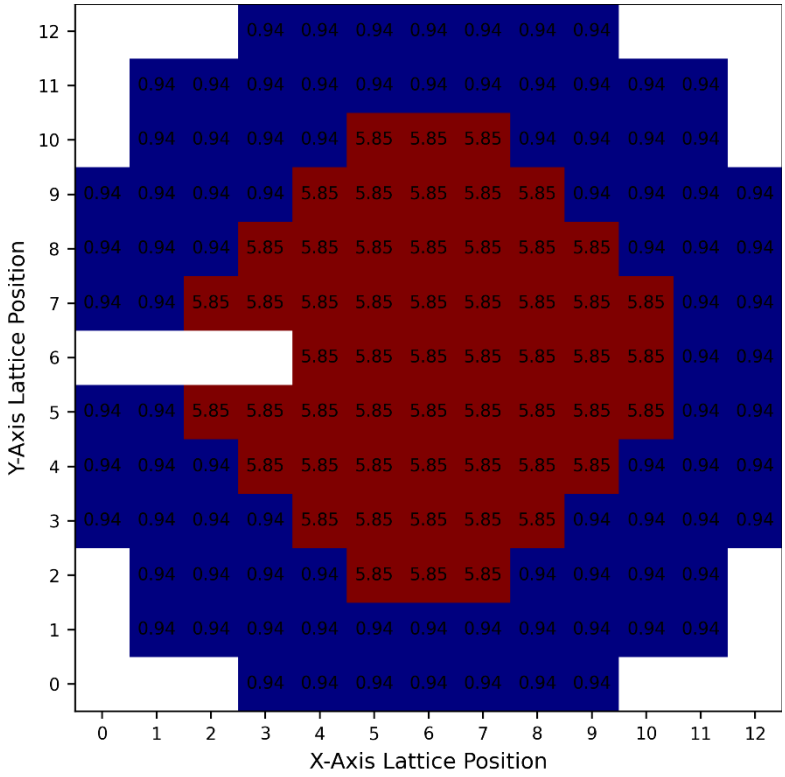

Figure 10. UTA–2 core fission power distribution at a peak overpower condition of 406.35 W for Case 3.

The subcooled margin was 45°C. The maximum LEU and natural uranium temperatures were 55.8 and 54.2°C, respectively. Scalar fields of temperature for Case 3 are presented in Figure 11 and Figure 12**.**

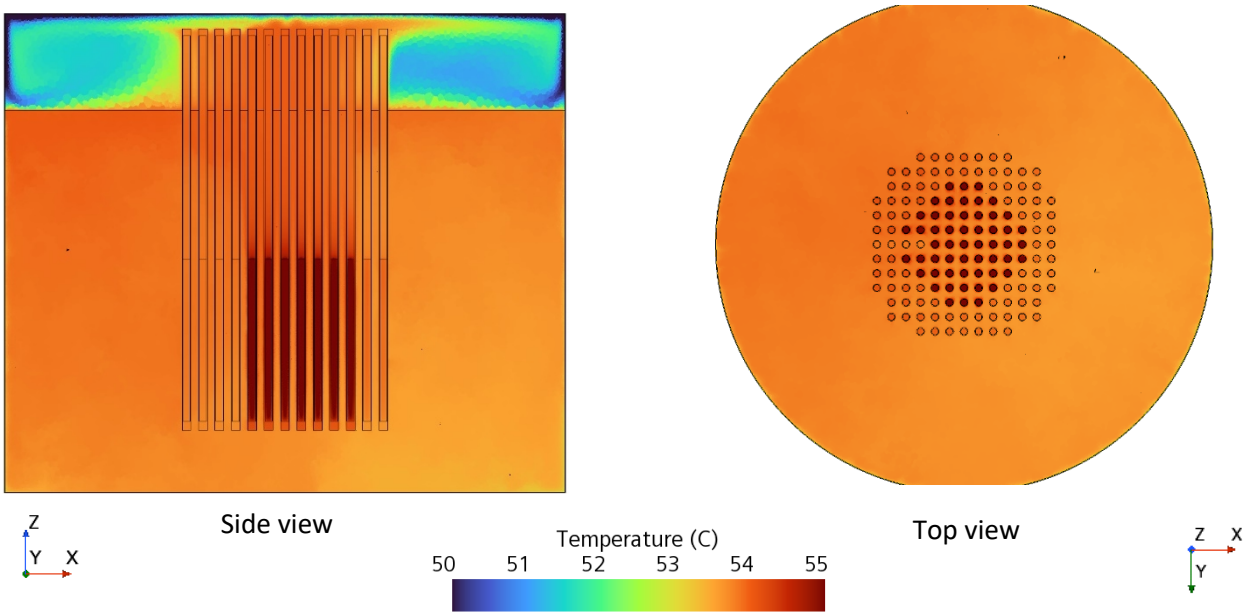

Figure 11. Side and top views of the UTA–2 subcritical assembly temperature field for Case 3 in which conduction and buoyancy-driven natural circulation combined methods were used for thermal energy transport at an overpower condition of 406 W.

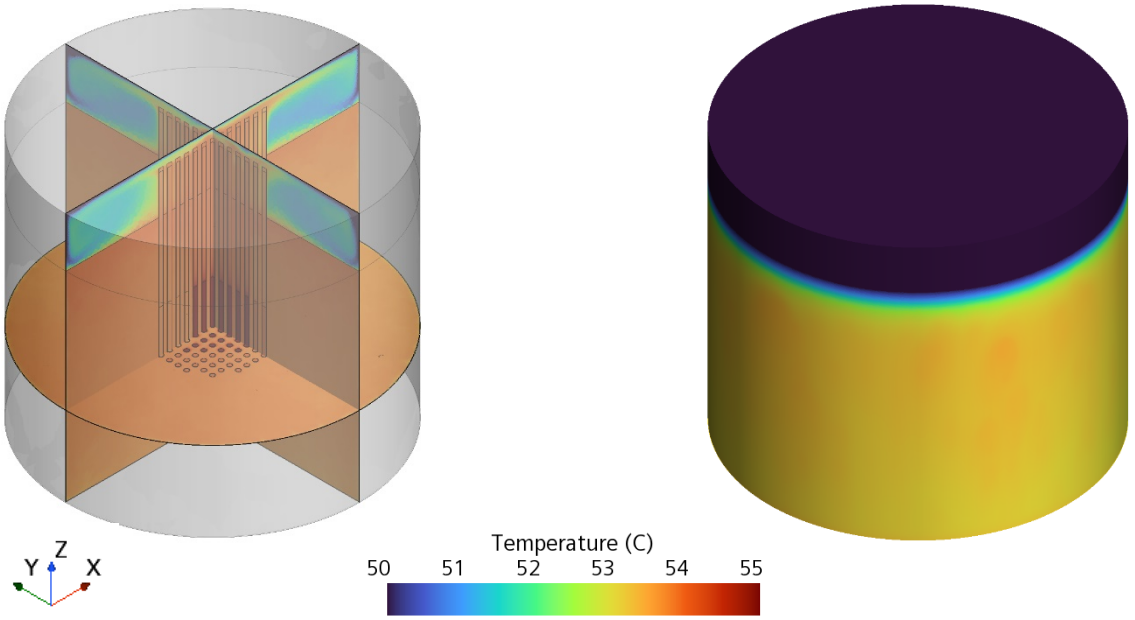

Figure 12. Isometric views of the UTA–2 subcritical assembly temperature field for Case 3 in which conduction and buoyancy-driven natural circulation combined methods were used for thermal energy transport at an overpower condition of 406 W.

3. CONCLUSION

Three cases were investigated in this work. Table 3 summarizes the numerical results of each case. Case 1 attempted to justify thermal margins using a simplified conduction-only approach. This overly conservative method yielded wetted cladding surface temperatures 63.8°C above the coolant saturation temperature.

Case 2 introduced the addition of buoyancy-driven natural circulation flow physics. Adding this coolant motion significantly distributed the thermal energy of the system via convective heat transfer. This relatively small amount of convective heat transfer significantly reduced system temperatures and increased the subcooled margin from –63.8 to 61.3°C. This margin confirmed that no boiling was expected during normal operation of UTA–2 at 230 W.

Case 3 studied the effect of an abnormal overpower event on the thermal margins during which the subcritical assembly power increased to 176% of nominal power, or 406 W. The subcooled margin was still 45°C and suggested that no boiling was expected during abnormal operation of UTA–2 at 406 W.

4. REFERENCES

[1] H. B. Awbi, "Calculation of convective heat transfer coefficients of room surfaces for natural circulation," *Energy and Buildings,* vol. 28, no. 1998, pp. 219-227, 1998.

[2] Z. Zhai and Q. Chen, "Numerical determination and treatment ofconvective heat transfer coeffcient in the coupled building energy and CFD simulation," *Building and Environment,* vol. 39, no. 2004, pp. 1001-1009, 2004.

[3] M. Glazoff, I. Rooyen, B. Coryell and C. Parga, "Comparison of Nuclear Fuels for TREAT: UO2 vs U3O8," INL/EXT-16-37972, Idaho Falls, ID, 2016.

[4] D. Stahl, "Fuels for Research and Test Reactors, Status Review: July 1982," ANL-83-5, Argonne, IL, 1982.

[5] The Aluminum Association, "Aluminum Standards and Data 2006," Arlington, 2006.

[6] Y. Touloukian, R. Kirby, R. Taylor and T. Lee, Thermophysical properties of matter, New York: Purdue Research Foundation, 1970.

[7] J. Keenan, J. Chao and J. Kaye, Gas Tables, Second Edition, John Wiley and Sons, Inc, 1980.

[8] International Association of the Properties of Water and Steam, "Revised Release on the IAPWS Industrial Formulation 1997 for the Thermodynamic Properties of Water and Steam," IAPWS Secretariat, 2007.

[9] L. F. Richardson, "The Approximate Arithmetical Solution by Finite Differences of Physical Problems Involving Differential Equations, with an Application to the Stresses in a Masonry Dam," *Philosophical Transactions of the Royal Society A,* vol. 210, pp. 307-357, 1911.

[10] L. F. Richardson and J. A. Gaunt, "The Deferred Approach to the Limit," *Philosophical Transactions of the Royal Society of London. Series A, containing papers of a mathematical or physical character,* vol. 226, pp. 299-361, 1927.